

Solid coin-like design activated carbon nanospheres derived from shallot peel precursor for boosting supercapacitor performance

by Rika Taslim

Submission date: 07-Oct-2021 01:59PM (UTC+0700)

Submission ID: 1667590354

File name: 1-s2.0-S2238785421010061-main.pdf (1.85M)

Word count: 7186

Character count: 40311



Available online at www.sciencedirect.com
jmr&t
Journal of Materials Research and Technology
journal homepage: www.elsevier.com/locate/jmrt



Original Article

Solid coin-like design activated carbon nanospheres derived from shallot peel precursor for boosting supercapacitor performance



Erman Taer^{a,*}, Apriwandi Apriwandi^a, Dhea Rama Andani^a,
Rika Taslim^{b,**}

^a Department of Physics, Faculty of Mathematic and Natural Sciences, University of Riau, Simpang Baru, Riau, 28293, Indonesia

^b Department of Industrial Engineering, State Islamic University of Sultan Syarif Kasim, Simpang Baru, Riau, 28293, Indonesia

ARTICLE INFO

Article history:

Received 8 August 2021

Accepted 6 September 2021

Available online 14 September 2021

Keywords:

Nanosphere

Nanofiber

Nanosheet

Electrode material

Supercapacitor

ABSTRACT

Thin porous carbon nanospheres based on natural materials, characterized by abundant availability, facile synthesis without templates, and heteroatom doping have confirmed the enhanced high performance of electrochemical energy storage devices. However, these potentials are difficult to obtain, and further poses a serious challenge. This work, activated carbon nanosphere was obtained from the biomass precursor shallot peel through a solid coin-like design with different chemical impregnations with high-temperature pyrolysis. The three different activators used were KOH, ZnCl₂, and NaOH, selected to optimize the precursor's potential to produce porous carbon nanospheres. All the carbons prepared exhibited potential nano-sized morphological structures with a high carbon content of 77.71–90.11%. Furthermore, the oxygen content of 24.60% indicated a doping heteroatom for the electrode material. Surprisingly, the KOH impregnation exhibited a nanosphere-rich morphological structure with a diameter of 102–124 nm adhering to the nanofiber surface. This combination of material properties has the benefit of improving the supercapacitor's performance with a high specific capacitance of 170.12 F g⁻¹ in a 1 M H₂SO₄ aqueous electrolyte. Meanwhile, the maximum specific energy reached 16.67 Wh kg⁻¹ with maximum specific power of 86.40 W kg⁻¹ at a constant current density of 1.0 A g⁻¹, in a two-electrode system. Therefore, the activated carbon with a solid coin-like design derived from shallot peel waste is a potential source of a rich nanospheres structure with a facile strategy for large-scale commercial electrochemical energy storage applications.

© 2021 The Authors. Published by Elsevier B.V. This is an open access article under the CC BY-NC-ND license (<http://creativecommons.org/licenses/by-nc-nd/4.0/>).

* Corresponding author.

** Corresponding author.

E-mail addresses: erman.taer@lecturer.unri.ac.id (E. Taer), rikataslim@gmail.com (R. Taslim).

<https://doi.org/10.1016/j.jmrt.2021.09.025>

2238-7854/© 2021 The Authors. Published by Elsevier B.V. This is an open access article under the CC BY-NC-ND license (<http://creativecommons.org/licenses/by-nc-nd/4.0/>).

1. Introduction

Rapid industrial and technological development plays an important role in changing the global community's social life. This has led to a significant increase in the use of high-end smartphones, tablets, laptops, personal computers, as well as high-quality cameras, and consequently, triggers high energy consumption, as well as environmental damage. Recently, researchers have focused on the procurement of environmentally friendly electrical technology and optimization of storage devices for electrical energy, particularly batteries, supercapacitors, and electrolytic capacitors. The hybrid electric vehicle model has been considered as one of the latest technological evolutionary progress initiating the intense study of energy storage devices with enhanced electrodes, especially lithium-ion batteries and high-performance supercapacitors [1,2]. In addition, supercapacitors are high-performance electrochemical storage devices with cheaper, as well as more effective, and efficient electrode materials, compared to lithium-ion batteries [3]. These devices also have considerably finite cycle life, high power density, excellent reversibility, and higher power density, and therefore, show promising application in various sectors, especially in electric vehicle systems [4,5]. The consumption of fuel oil and natural gas for industrial vehicles and machinery leads to environmental pollution, followed by the depletion of these non-renewable resources, and also shows the need to develop high-performance supercapacitors based on inexpensive, easily synthesized, as well as highly effective electrode materials. Numerous raw materials have been studied to obtain superior electrodes for supercapacitors, including polymers [6,7], graphene oxide [8], metal oxides [9–11], carbon black [12], and biomass-based porous carbon [13,14]. However, biomass-based carbon is cheap, easy to obtain, abundantly available, as well as pollution-free, and is, therefore, more popular, compared to the other materials [15]. Furthermore, this is a suitable alternative solution to reduce toxic waste from the by-products of industrial activities [16,17]. Recently, agricultural by-products have shown outstanding supercapacitor performance, obtaining surface areas of up to $>2000 \text{ m}^2\text{g}^{-1}$, and this is able to improve the specific capacitance properties by about 400 Fg^{-1} [18–20]. Most importantly, the specific energy is increasable by up to 3 times, compared to the review studies by optimizing pore characteristics by hierarchically interconnecting 3D pores between micro, meso, and macropores [20,21]. This is the answer to the main challenge of supercapacitor-related studies where the specific energy was reported to be lower, compared to the specific power. However, not all biomass is able to produce a 3D hierarchical pore structure including micro, meso, and macropores. Also, the material's benefits are limited by the relatively complex preparation methods using templates, metal frameworks, and the addition of synthetic materials. Researchers believe this challenge is bound to be overcome by changing the particle size and up to nano size. Furthermore, carbon nanospheres have shown high specific surface area advantages, providing well-connected diverse pore structures, high conductivity, as well as good chemical-thermal stability, and this is able to promote high specific energies in electrochemical energy

storage devices [22,23]. Zheng et al., (2021) reported the superiority of the nanosphere's structure has the capacity to increase the specific energy to 71.9 Whkg^{-1} , with a specific capacitance of 273.9 Fg^{-1} [24]. Zhou et al., (2021) also reported a similar finding, with an ultra-high specific capacitance of 1214 Fg^{-1} [25]. However, these studies mostly used polymeric materials as well as metal oxides for fabrication, and the method presented is relatively complex, requires various instruments, and has toxic side effects. Recently, He et al., (2021) studied the potential of red rod biomass waste in producing hierarchically porous hollow carbon nanospheres through a one-step by thermal treatment, and reported a surface area of $1792 \text{ m}^2\text{g}^{-1}$, with a specific capacitance of 198.6 Fg^{-1} [26]. In addition, the method reported is relatively simple, and reproducible with standard instruments. This confirms natural materials are a potential source of nanosphere structures, although this is not confirmed in all biomass.

In this study, porous carbon nanospheres were produced from shallot peel agricultural waste through a simple and feasible strategy with chemical impregnation of KOH, ZnCl_2 , and NaOH at high-temperature pyrolysis. Several chemical activations were applied to optimize the precursor's potential morphological structure. The porous carbon was prepared in the form of an adhesive-free solid with a coin-like design as a basic approximation to maintain the real conductivity properties, and the porous carbon obtained possessed a nanosphere structure followed by nanofibers and nanosheets with a specific surface area of $1182.3 \text{ m}^2\text{g}^{-1}$. Most importantly, the KOH impregnation produced a nanosphere-rich morphological structure with a diameter of 102–124 nm adhering to the nanofiber surface. The supercapacitor cell system's high electrochemical properties were confirmed with a specific capacitance of 170 Fg^{-1} at a current density of 1.0 Ag^{-1} , through a two-electrode configuration. Meanwhile, the maximum specific energy was discovered to reach 16.67 Whkg^{-1} , with a maximum specific power of 86.40 Wkg^{-1} in $1 \text{ M H}_2\text{SO}_4$ aqueous electrolyte. Therefore, environmentally friendly, inexpensive, and controlled carbon nanospheres were obtained from shallot peel biomass precursors as electrode material for high-performance electrochemical energy storage devices, using a chemical impregnation method at high-temperature pyrolysis.

2. Materials and methods

2.1. Materials

The selected biomass raw material was shallot peels waste obtained from vegetable farmers in Pekanbaru city. Subsequently, the samples were dried in two stages: under direct sunlight and in an oven vacuum at 110°C . This was followed by crushing and grinding the dried shallot peels into powder with particle size $<60 \mu\text{m}$. Meanwhile, the chemical activating agents used, KOH, ZnCl_2 , and NaOH in a 0.5 mL^{-1} solution, were purchased from several brands including Sigma Aldrich and Merck KGaA, respectively. In the electrochemical analysis, the electrolyte prepared was a $1 \text{ M H}_2\text{SO}_4$ solution obtained from Panreac Quimica Sau while the separator was

selected from the organic material of the duck eggshell cell membrane.

2.2. Synthesis of shallot peel-based nanospheres activated carbon

For this experiment, 30g of Shallot peel (SP) powder were chemically impregnated separately, using KOH, ZnCl_2 , and NaOH solutions, then oven-dried at 110°C for 36–48 h. The chemically impregnated carbon powder was then converted to a solid coin-like shape by passing through a hydraulic press instrument under a pressure equivalent to a load of $\pm 8\text{ton}$. This solid coin-like design was prepared without the addition of adhesives, by purely optimizing the raw material's self-adhesive. A total of 15 solid coin-like carbon were then placed into a furnace tube for high-temperature pyrolysis involving carbonization and physical activation processes in the N_2 and CO_2 gas environments. The optimum temperatures for carbonization and physical activation at 600°C with a temperature increase of $3^\circ\text{C}/\text{min}$ and 900°C with a temperature increase of $10^\circ\text{C}/\text{min}$, respectively. Subsequently, all samples were neutralized by immersion in DI water.

2.3. Material characterization

The density of samples designed to possess a solid coin-like shape without the use of adhesive materials must be evaluated through measurements of mass, diameter, and thickness. In this study, the microcrystalline phase change behavior was analyzed by X-ray diffraction (Shimadzu-XRF-7000L) at a 2θ angle range of $10\text{--}60^\circ$ with $\text{CuK}\alpha$ as the irradiation source, while the microcrystalline dimensions were evaluated using the Debye-Scherrer equation [27]. Furthermore, the material's morphology and surface structure were analyzed using the scanning electron microscopy method at a maximum voltage of 15Kv (JSM-6510A/JSM-6510LA), while the elemental composition was confirmed using energy dispersive spectroscopy in the energy range of $0\text{--}20\text{keV}$ (JSM-6510A/JSM-6510LA).

2.4. Confirmation of electrochemical properties

The electrochemical properties of nanospheres activated carbon based on shallot peel waste were evaluated through the general cyclic voltammetry (CV) and galvanostatic charge-discharge (GCD) technique. Furthermore, the supercapacitor cell was prepared in a two-electrode configuration comprising two solid coin-like activated carbons designed without adhesive and separated by an organic separator in an aqueous electrolyte solution of $1\text{M H}_2\text{SO}_4$, with a working mass of $\pm 0.0101\text{g}$. The cyclic voltammetry method was performed at a maximum potential window of $0\text{--}1\text{V}$ in several scan rates including $1, 2, 5$, and 10 mV s^{-1} , and the specific capacitance was evaluated using the standard equation [28,29]. Also, the galvanostatic charge discharge was evaluated at a constant current density of 1.0 A g^{-1} , while the specific capacitance, specific energy, and specific power were determined using standard equations [30].

3. Results and discussions

3.1. Materials properties analysis

Density change is an initial analysis performed to evaluate the material properties of the activated carbon designed to resemble a solid coin without any adhesive material. The chemical impregnation processes using KOH, ZnCl_2 , and NaOH treatments at high-temperature pyrolysis directly affect the coin's density through reduced mass, thickness, and diameter. The high-temperature pyrolysis and a certain temperature rise led to evaporation of the water content, volatile elements, and other light compounds [31]. Generally, Shallot peel as raw material contains hemicellulose, cellulose, as well as lignin compounds incorporated in the lignocellulosic components, and this undergoes decomposition, as well as reduction at different temperatures. Furthermore, the carbonization process in an N_2 gas environment at a maximum chamber temperature of 600°C is able to produce carbon fixed from precursor samples through evaporation of the water content and reduction of the lignocellulosic components, consequently, reducing the sample's density [32]. However, the residual content of tar as a by-product of carbonization is considered to hinder optimized carbon pores framework expansions, therefore, further physical activation processes are required in a CO_2 gas environment [33]. According to Fig. 1, the physical activation process was performed at $600^\circ\text{C}\text{--}900^\circ\text{C}$ to reduce as well as degrade cellulose and lignin compounds, maximizes pore expansion, while opening narrow pores on the activated carbon surface, consequently, reducing the activated carbon's density [34]. The three shallot peel-based activated carbon samples experienced a reduction in density after a high-temperature pyrolysis process, including carbonization and physical activation integrated into one step. Before the pyrolysis, the densities of activated carbon of the SP-KOH, SP- ZnCl_2 , and SP-NaOH samples were 0.8890 , 1.0946 , as well as 0.8075 g cm^{-3} , respectively, and after the pyrolysis, the densities were 0.8455 , 0.8489 , and 0.5889 g cm^{-3} , respectively. The largest density

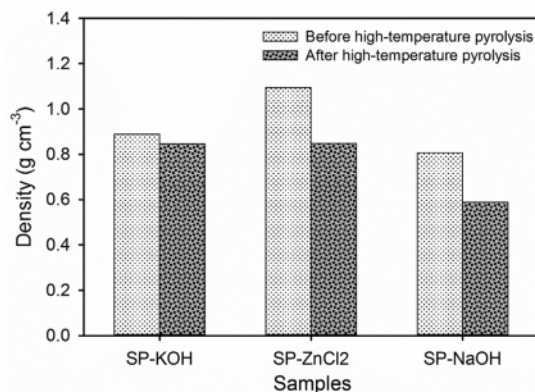


Fig. 1 – Change in density of coinlike porous carbon nanosphere.

reduction of 27.07% was obtained in the SP-NaOH sample, followed by the SP-ZnCl₂ and SP-KOH samples at 22.44% and 4.89%, respectively. Therefore, chemical activation also significantly affects the sample's density, due to the activating reagents' features and reactions with carbon at different temperatures. This study's density analysis is in agreement with previously reported studies using different precursors, including reed waste [35], and durian shell [36].

Fig. 2 shows the X-ray diffraction analysis on the microcrystalline phases of the three activated carbons obtained. The XRD pattern for the SP-KOH, SP-ZnCl₂, and SP-NaOH samples was evaluated at an angle range of 10°–60°. Generally, all samples showed two broad peaks at $2\theta = 24^\circ$ and 45° , followed by several sharp peaks at different angles. The broad peaks at $2\theta = 24^\circ$ and 45° correlated with the scattering planes 002 and 100, confirming the turbostratic disturbed carbon structure and leading to desirable amorphous properties [37]. This property helps the electrode material to provide an ionic charge contact area in optimizing the supercapacitor's high performance. In addition, the SP-KOH sample displayed two larger broad peaks, compared to the SP-ZnCl₂ and SP-NaOH samples, especially in the 002 reflection plane. This is probably due to the carbon surface's increasingly irregular structure, initiating the formation of various pore sizes [38]. This is in agreement with several case studies, where similar cases were also reported [39]. Also, sharp peaks were found at different angles, including 28.1–29.4°, 33.1°, 37.6°, 45.8–46.3°, and 48.8°, confirming the presence of crystalline compounds in almost all samples, particularly CaO/CaCO₃, MgO, and SiO₂ compounds. CaO/CaCO₃ compounds were found at 28.1–29.4°, and 48.8° (JCPDS No. 82-1690), while MgO compounds were confirmed at 45.8–46.3°, and SiO₂ compounds at 33.1° and 37.6° (JCPDS No. 89-1668). The presence of these compounds is partially due to basic constituents of the biomass precursors subjected to oxidative stress during pyrolysis. These results were also confirmed through elemental analysis using EDS.

Table 1 provides a detailed summary of the interlayer spacing d_{002} – d_{100} and microcrystalline dimensions L_c – L_a for chemically impregnated activated carbon. The d_{002} and d_{001} values of SP-KOH, SP-ZnCl₂, and SP-NaOH are reasonable for

bio-waste-based amorphous carbon. Furthermore, d_{002} has a relatively higher value of 9.09%, compared to d_{002} for normal graphite, confirming the irregular (turbostratic) carbon structure. Meanwhile, the microcrystalline dimensions, especially L_c , are closely related to the prediction of the specific surface area of carbonaceous materials through empirical equations $SSA_{XRD} = 5^{0.9} L_c$, as previously reported [40,41]. L_c is a parameter inversely proportional to the specific surface area, therefore, a low L_c implies a high surface area. The least L_c value was obtained in the SP-KOH sample, indicating the specific surface area was predicted to reach 1182.23 m² g^{−1}, while the SP-ZnCl₂ and SP-NaOH counterparts were 1058.58 m² g^{−1} and 597.78 m² g^{−1}, respectively. Table 1 presents the detailed summary of the SSA_{XRD} properties for the three samples. These properties are required to improve the electrode material's electrochemical properties for electrochemical energy storage applications.

The coin-like activated carbon's morphological structure was evaluated using scanning electron microscopy. Fig. 3 shows the SEM image for the chemically impregnated green shallot-based activated carbon samples of KOH, ZnCl₂, and NaOH. According to the diagram, the samples retained the basic structure of the biomass-based precursors, and exhibited the morphology as well as structure of nanospheres and nanofibers, with relatively varied sizes, mainly due to the difference in the activating chemical agents. In the carbonization and high-temperature activation processes, the chemical reagent dehydrates and degrades the complex lignocellulosic compounds with the ability to reveal unique structures and morphology on the sample [42]. The Lignin component contributes to the appearance of tubular structures and is speculated to present nanospheres on porous carbon-based biomass [42]. Meanwhile, the cellulose degraded due to high temperature contributes to the nanofiber structure [43]. Fig. 3a shows the KOH impregnated samples displayed a distinct surface morphology rich in nanospheres dotted with nanofibers. The nanosphere's diameter ranges from 102 nm to 124 nm, while the fiber diameter ranges from 135 to 370 nm. In the selected magnification area, the nanospheres are seen to adhere to almost all the fiber surfaces, and are closely inter-related, initiating hierarchically connected pore channels while minimizing agglomeration, and consequently, ensuring more effective ion contact sites and charge transport pathways for electrochemical energy storage [24]. Fig. 3b shows the ZnCl₂ impregnated sample, confirming the rod-like morphological structure with a diameter of 362–882 nm and a predominant clump of carbon blocks. The nanofibers with a diameter of 168–196 nm were also confirmed to be clear in relatively small amounts, compared to the SP-KOH samples, while the nanospheres with a diameter of 161–128 nm, were confirmed to adhere to the fiber's surfaces, although in relatively small amounts. In addition, the activation of ZnCl₂ is speculated to be able to reduce the structure of nanospheres and nanofibers. At pyrolysis temperatures of >500 °C, ZnCl₂ reacts with the carbon matrix framework to produce oxidative compounds [44]. Numerous functional groups containing oxygen in the nano-spherical structure are evaporated by ZnCl₂ in the form of H₂O and CO, consequently, reducing the number of nanospheres on the sample's surface morphology [45]. Furthermore, the byproduct of the chemical reaction in the

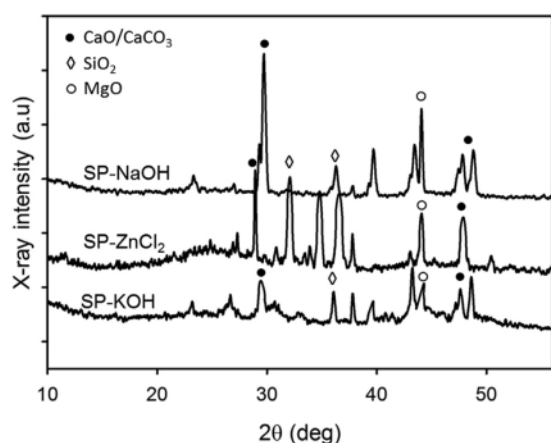


Fig. 2 – XRD pattern of coinlike porous carbon nanosphere.

Table 1 – The interlayer spacing, dimension microcrystalline and specific surface area of coinlike porous carbon nanosphere.

Samples	$2\theta_{002}$ (°)	$2\theta_{100}$ (°)	d_{002} (Å)	d_{100} (Å)	L_c (Å)	L_a (Å)	SSA_{XRD}
SP-KOH	25.453	44.260	3.596	2.044	8.042	49.177	1182.23
SP-ZnCl ₂	24.241	43.499	3.668	2.078	9.161	16.707	1058.58
SP-NaOH	23.431	42.037	3.499	2.147	15.482	39.858	597.78

form of ZnO simultaneously erodes the carbon sphere, producing mostly micropores in the nano-spherical structure. However, this is able to simultaneously cause the collapse of large carbon nanospheres to form carbon blocks, and causes a smaller diameter in the nanofiber structure, compared to the SP-KOH sample. This structure has the capacity to increase the electrode material's conductivity and improve the supercapacitor's capacitive properties [46].

Fig. 3c shows the SP-NaOH sample's morphology with relatively confirmed short nanofiber structures of 78–250 nm diameter, as well as a unique flower-like structure. In the selected magnification area, the SP-NaOH sample exhibits a sheet structure with a thickness of 26–56 nm. The NaOH reaction at high-temperature pyrolysis is able to maintain the

basic structure of the cellulose precursor, Na₂CO₃ as the reaction's first product, to initiate the formation of oxidative compounds NaO₂ by evaporating CO and H₂O compounds [47]. This is able to decompose the lignocellulosic material's carbon framework and maintain the structure of the fibers and sheets in the sample [48]. Also, this combination of structures has greatly contributed to discovering the ideal material for high-performance supercapacitor electrodes [49].

Table 2 presents a detailed summary of the elemental status of shallot peel-based activated carbon with different chemical impregnations. Generally, the three samples confirmed carbon had the highest elemental percentage of about 77.71%–90.11%. This showed chemical impregnation at high-temperature pyrolysis in N₂ and CO₂ environments

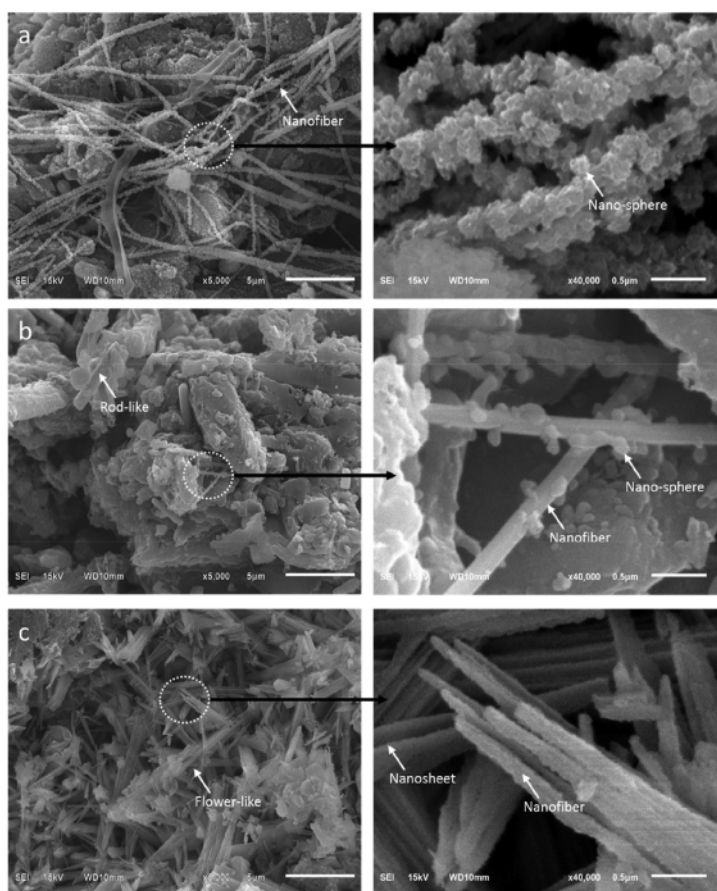
**Fig. 3 – SEM image of (a) SP-KOH, (b) SP-ZnCl₂, dan (c) SP-NaOH.**

Table 2 – Elemental analysis of coinlike porous carbon nanosphere.

Samples	Element analysis					
	C (%)	O (%)	Mg (%)	Ca (%)	Si (%)	K (%)
SP-KOH	77.71	18.60	1.04	1.91	0.51	0.23
SP-ZnCl ₂	69.18	24.74	0.91	4.83	0.29	0.05
SP-NaOH	90.11	8.57	0.41	0.62	0.26	0.03

successfully converted biomass precursors into high purity carbon. The SP-NaOH sample produced the highest carbon of 90.11% followed by the SP-KOH sample, and SP-ZnCl₂ 77.71% and 69.11%, respectively. Therefore, the provision of electron and ion charge active surface sites to form a high electrochemical double-layer is highly beneficial. Meanwhile, oxygen had the second-highest elemental percentages ranging from 18.60% to 24.74%. This indicates the presence of oxidative compounds, for instance, CaO/CaCO₃, MgO, and SiO₂ in all samples. These results are confirmed to be the same as the previously discussed XRD pattern analysis. This elemental oxygen tends to provide wettability properties for ions to diffuse at the electrode/electrolyte interface [50]. Also, other contaminants including Mg, Ca, Si, and K are present in oxidative compounds in relatively minute amounts, due to the basic biomass components partially decomposed during the high-temperature pyrolysis process [51].

3.2. Electrochemical behavior analysis

The electrochemical properties of supercapacitor cells were confirmed through cyclic voltammetry and galvanostatic charge–discharge techniques in a two-electrode configuration system. Supercapacitor cells were prepared in the form of a sandwich layer with activated carbon in a coin-like design, without the addition of adhesives, including PVP or PFDV. The electrolyte selected was aqueous electrolyte 1M H₂SO₄, while the organic separator used was derived from duck eggshell membrane. Fig. 4 shows cyclic voltammetry profiles for all three samples evaluated at a scan rate of 1 mVs⁻¹. The image shows a distorted rectangular shape indicating the relatively ideal electrochemical double-layer properties of porous carbon-based biomass [52]. Furthermore, the high oxygen content of 24.70% contributed to the sample's wettability, and this possibly exerted a pseudocapacitance effect on the sample [53]. This profile has not been completely confirmed, however, this is faintly visible in the SP-KOH sample, where a slight surge current density in the voltage range of 0.2–0.6V occurred. The area sweep of the closed hysteresis loop also confirmed the electrode material's capacitive behavior, where the largest hysteresis loop was found in the SP-KOH samples and exhibited the highest capacitive property, followed by SP-ZnCl₂ and SP-NaOH. Based on standard equation, the SP-KOH, SP-ZnCl₂, and SP-NaOH samples had specific capacitances of 151, 116, and 91 Fg⁻¹, respectively.

The thin diameter nano-spherical structure allows the carbon matrix framework to exhibit a high specific surface area of 1182.23 m²g⁻¹ and a variety of pore structures in the <50 nm size range, therefore, enabling rich micropores and mesopores in activated carbon [24]. The high surface area

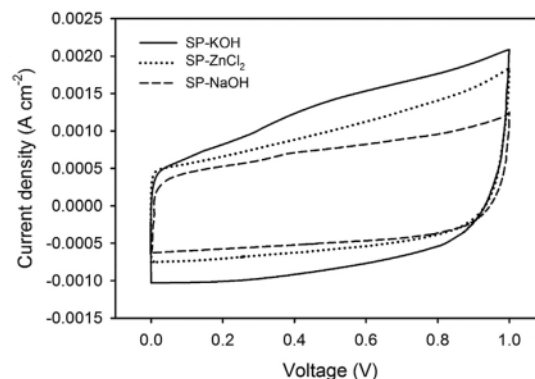


Fig. 4 Cyclic voltammogram of SP-KOH, SP-ZnCl₂, and SP-NaOH at scan rate of 1 mV s⁻¹.

initiated by the micropores structure contributes to the provision of an active site for the charge diffusion of the electrolyte ions on the electrode surface [20]. In addition, the mesopores confirm the larger charge-carrying channel and consequently, low internal resistance. This combination significantly increases the electrode material's specific capacitance as shown in the SP-KOH sample, while the nanofibers structure is responsible for the high conductivity [54]. The electrodes' performances were also evaluated through differences in scanning rates. Fig. 5a–c shows the SP-KOH, SP-ZnCl₂, and SP-NaOH samples displayed CV curves at scan rates of 1, 2, and 5 mV s⁻¹. The CV profile also forms a distorted rectangular curve indicating normal EDLC behavior, and a quicker saturation rate. The application of the scanning rate also significantly affects the electrode's capacitive properties. According to Fig. 5d, the specific capacitance is reduced at higher scan rates to 10 mVs⁻¹, confirming the uncontrolled pore structure hindering the transport of electrolyte ions on the electrode surface. SP-ZnCl₂ does not possess the highest capacitive properties as well as specific surface area, however, the sample is able to maintain the highest specific capacitance of about 67.4% at a high scanning rate of 10 mVs⁻¹. This is due to the presence of a nanofiber structure contributing to increased conductivity, and consequently maintain the electrochemical properties [54].

Fig. 6 shows all samples exhibited a perturbed isosceles triangular GCD profile at a constant current density of 1.0 Ag⁻¹, confirming the normal double-layer electrochemical properties, and this is consistent with the CV curve shown in Fig. 4. Also, the iR drop was found to be insignificantly indicative of relatively low resistance in the electrode material. The charging and discharging times in the GCD profile significantly confirm the supercapacitor cell's performance, with the longest discharge time obtained in SP-KOH samples, indicating the highest capacitive properties, followed by SP-ZnCl₂ and SP-NaOH samples. Based on standard formula, the specific capacitances obtained for SP-KOH, SP-ZnCl₂, and SP-NaOH samples are 170.12, 127.4, as well as 79.2 Fg⁻¹, respectively, and these values correspond to the data obtained from the CV technique.

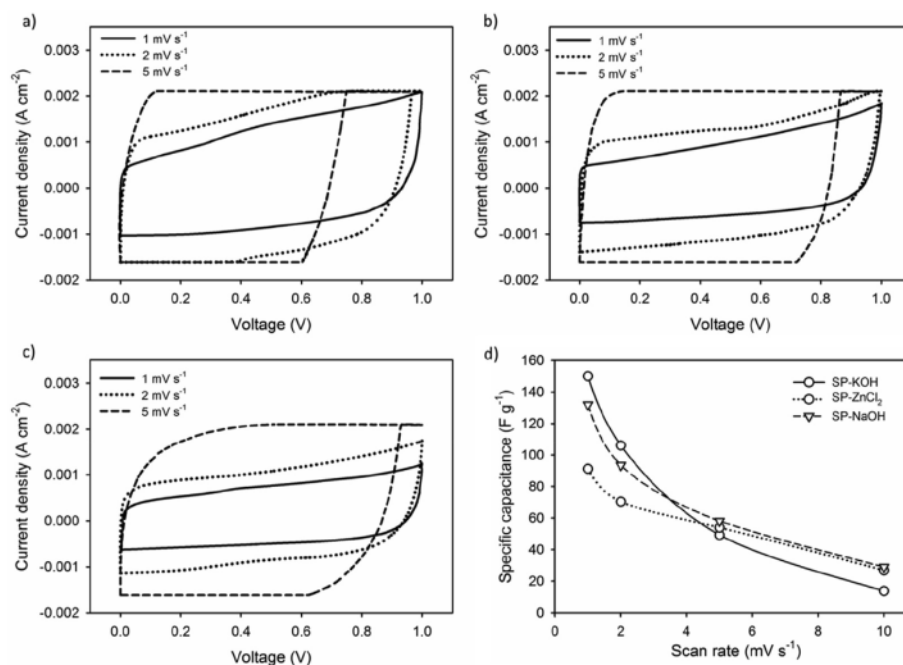


Fig. 5 – CV voltammogram at different scan rate of (a) SP-KOH, (b) SP-ZnCl₂, (c) SP-NaOH, and (d) specific capacitance vs. scan rate.

In addition, SP-KOH has superior material properties compared to the other two samples, especially the morphology and structure of thin nanospheres followed by nanofibers with higher specific surface area. This combination of nano-sized structures allows the formation of diverse pores, therefore, imparting high microporosity as well as mesoporosity properties in the sample, and this leads to a high surface area and larger ion diffusion pathway, consequently, improving the supercapacitor's performance [55]. In this study, the presence of thin diameter nanospheres in SP-KOH samples resulted in the relatively higher internal

resistance of 31 mΩ, compared to the SP-ZnCl₂ and SP-NaOH counterparts of 22 mΩ and 10 mΩ, respectively. The presence of thin diameter nanospheres allows a more dominant distribution of small pores and provides more electron/ion active sites at the electrolyte/electrode interface [23,26]. However, this in turn often significantly narrows the ionic charges' migration path, consequently, increasing the internal resistance. In contrast to the SP-NaOH samples, the presence of a nanosheet structure is able to shorten the ions' migration path significantly, therefore, enabling free diffusion without interference at the electrolyte/electrode interface, while

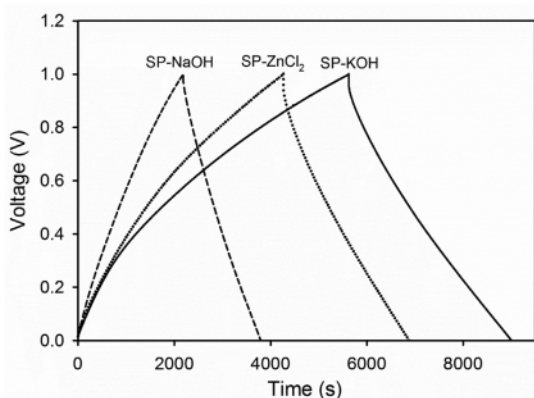


Fig. 6 – GCD profile of SP-KOH, SP-ZnCl₂, and SP-NaOH at current density of 1.0 A g⁻¹.

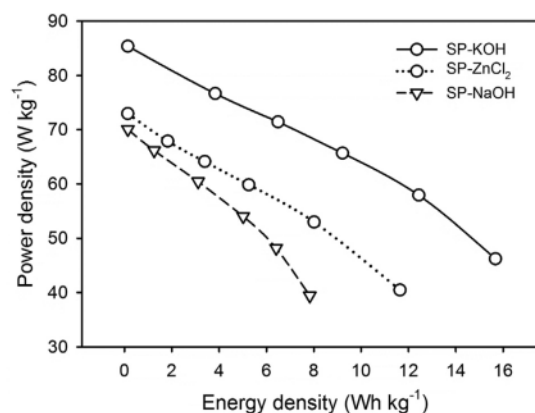


Fig. 7 – Ragone plot of energy specific and power density of coinlike porous carbon nanosphere.

47
Table 3 – Comparison of electrochemical properties of various sources of electrode materials.

Sources	Structures	20 A (m ² g ⁻¹)	Electrode type	C _{sp} (F g ⁻¹)	Electrolyte	E (Wh kg ⁻¹)	P (W kg ⁻¹)	R (Ω)	refs
Reed rod	Nanosphere	1792	powder	198.6	6 M KOH	3.5	20k	0.29	[26]
Glucose	Nanosphere	1210	Powder	282	6 M KOH	8.5	250	1.04	[22]
Pyrrole-based	Nanosphere	1347	Powder	395	6 M KOH	—	—	0.77	[23]
Nickel and Cobalt MOF-derived	Microsphere	1135	Powder	1214	2 M KOH	55.4	758.5	0.93	[25]
Quinone-amine polymer	Nanosphere	2671.2	Powder	273.9	6 M KOH	8.0	80.3	—	[24]
American poplar fruit	Tubular-like	942	Coin-type	58.71	6 M KOH	7.99	372	1.97	[56]
Cassava petiole	Rod-like	759.81	Monolith	193.68	1 M H ₂ SO ₄	26.90	96.94	—	[39]
Shallot peel	Nanosphere	1182.2	Coinlike	170.12	1 M H ₂ SO ₄	16.67	86.40	0.031	This work

producing the least internal resistance, as reported in previous studies [49].

The specific energy and specific power of the shallot peel-based activated carbon were evaluated using standard equations (Fig. 7). The Ragone plot shows the highest specific energy of 16.67 Whkg⁻¹ found in the S-12OH sample with a maximum specific power of 86.40 Wkg⁻¹ at a constant current density of 1.0 Ag⁻¹, followed by SP-ZnCl₂ and SP-NaOH samples with specific energies of 12.64 and 8.82 Whkg⁻¹ at the maximum specific power of 73.96 and 71.07 Wkg⁻¹, respectively. According to Table 3, the maximum specific energy obtained in this study is considerably greater, compared to other reports where relatively complex methods requiring synthetic base materials were used.

4. Conclusion

Biomass waste of shallot peel-based activated carbon nanospheres was successfully prepared using a solid coin-like design and impregnation with different chemicals at high-temperature pyrolysis. Furthermore, three chemical activating agents were selected to maximize the precursors' potential to produce nano-sized structures. All samples were confirmed to possess relatively adequate amorphous properties for biomass-based porous carbon. Each activator significantly produces different nanostructures including nanospheres, followed by nanofibers and nanosheets. SP-KOH exhibits a morphological structure rich in thin nanospheres adhering tightly to the nanofiber surface, while SP-ZnCl₂ consistently displays nanofiber morphology with reduced nanospheres. Interestingly, SP-NaOH provides a favorable nanosheet structure to reduce the electrode material's resistance. The combination of these nanostructural properties is able to increase the material's specific capacitance by 170.12 F g⁻¹ in the 1 M H₂SO₄ electrolyte. These results confirm the solid coin-like design of the activated carbon of the onion peel is a remarkable innovation to obtain high-performance electrode materials for energy storage applications.

Declaration of Competing Interest

The authors declare that they have no known competing financial interests or personal relationships that could have appeared to influence the work reported in this paper.

Acknowledgement

The work was financially supported by Kementerian Pendidikan, Kebudayaan, Riset, dan Teknologi, Republic of Indonesia through first year Project of world Class Research (WCR) contract No. 1393/UN.19.5.1.3/PT.01.03/2021.

REFERENCES

- [1] Sharma P, Bhatti TS. A review on electrochemical double-layer capacitors. *Energy Convers Manag* 2010;51:2901–12. <https://doi.org/10.1016/j.enconman.2010.06.031>.
- [2] Chen T, Dai L. Carbon nanomaterials for high-performance supercapacitors. *Mater Today* 2013;16:272–80. <https://doi.org/10.1016/j.mattod.2013.07.002>.
- [3] Mensah-Darkwa K, Zequine C, Kahol PK, Gupta RK. Supercapacitor energy storage device using biowastes: a sustainable approach to green energy. *Sustain* 2019;11. <https://doi.org/10.3390/su11020414>.
- [4] Poonam Sharma K, Arora A, Tripathi SK. Review of supercapacitors: materials and devices. *J Energy Storage* 2019;21:801–25. <https://doi.org/10.1016/j.est.2019.01.010>.
- [5] González A, Goikolea E, Barrena JA, Mysyk R. Review on supercapacitors: technologies and materials. *Renew Sustain Energy Rev* 2016;58:1189–206. <https://doi.org/10.1016/j.rser.2015.12.249>.
- [6] Wu ZY, Liang HW, Chen LF, Hu BC, Yu SH. Bacterial cellulose: a robust platform for design of three dimensional carbon-based functional nanomaterials. *Acc Chem Res* 2016;49:96–105. <https://doi.org/10.1021/acs.accounts.5b00380>.
- [7] Miller EE, Hua Y, Tezel FH. Materials for energy storage: review of electrode materials and methods of increasing capacitance for supercapacitors. *J Energy Storage* 2018;20:30–40. <https://doi.org/10.1016/j.est.2018.08.009>.
- [8] Shen W, Zang J, Hu H, Xu J, Zhang Z, Yan R, et al. Controlled synthesis of KCu₇S₄/rGO nanocomposites for electrochemical energy storage. *Mater Des* 2020;195:108992. <https://doi.org/10.1016/j.matdes.2020.108992>.
- [9] Bai Y, Liu R, Li E, Li X, Liu Y, Yuan G. Graphene/Carbon Nanotube/Bacterial Cellulose assisted supporting for polypyrrole towards flexible supercapacitor applications. *J Alloys Compd* 2019;777:524–30. <https://doi.org/10.1016/j.jallcom.2018.10.376>.
- [10] Dai S, Bai Y, Shen W, Zhang S, Hu H, Fu J, et al. Core-shell structured Fe₂O₃@Fe₃C@C nanochains and Ni–Co carbonate hydroxide hybridized microspheres for high-performance battery-type supercapacitor. *J Power Sources* 2021:482. <https://doi.org/10.1016/j.jpowsour.2020.228915>.

- [11] Dai S, Zhang Z, Xu J, Shen W, Zhang Q, Yang X, et al. In situ Raman study of nickel bicarbonate for high-performance energy storage device. *Nanomater Energy* 2019;64:103919. <https://doi.org/10.1016/j.nanoen.2019.103919>.
- [12] Young C, Park T, Yi JW, Kim J, Hossain MSA, Kaneti YV, et al. Advanced functional carbons and their hybrid nanoarchitectures towards supercapacitor applications. *ChemSusChem* 2018;11:3546–58. <https://doi.org/10.1002/cssc.201801525>.
- [13] Wan L, Song P, Liu J, Chen D, Xiao R, Zhang Y, et al. Facile synthesis of nitrogen self-doped hierarchical porous carbon derived from pine pollen via MgCO₃ activation for high-performance supercapacitors. *J Power Sources* 2019;438:227013. <https://doi.org/10.1016/j.jpowsour.2019.227013>.
- [14] Jiang X, Guo F, Jia X, Zhan Y, Zhou H, Qian L. Synthesis of nitrogen-doped hierarchical porous carbons from peanut shell as a promising electrode material for high-performance supercapacitors. *J Energy Storage* 2020;30:101451. <https://doi.org/10.1016/j.est.2020.101451>.
- [15] Gao Z, Zhang Y, Song N, Li X. Biomass-derived renewable carbon materials for electrochemical energy storage. *Mater Res Lett* 2017;5:69–88. <https://doi.org/10.1080/21663831.2016.1250834>.
- [16] Li Y, Wang X, Cao M. Three-dimensional porous carbon frameworks derived from mangosteen peel waste as promising materials for CO₂ capture and supercapacitors. *J CO₂ Util* 2018;27:204–16. <https://doi.org/10.1016/j.jcou.2018.07.019>.
- [17] Wei H, Wang H, Li A, Li H, Cui D, Dong M, et al. Advanced porous hierarchical activated carbon derived from agricultural wastes toward high performance supercapacitors. *J Alloys Compd* 2020;820:153111. <https://doi.org/10.1016/j.jallcom.2019.153111>.
- [18] Sun K, Yu S, Hu Z, Li Z, Lei G, Xiao Q, et al. Oxygen-containing hierarchically porous carbon materials derived from wild jujube pit for high-performance supercapacitor. *Electrochim Acta* 2017;231:417–28. <https://doi.org/10.1016/j.electacta.2017.02.078>.
- [19] Zhang J, Chen H, Bai J, Xu M, Luo C, Yang L, et al. N-doped hierarchically porous carbon derived from grape marcs for high-performance supercapacitors. *J Alloys Compd* 2021;854:157207. <https://doi.org/10.1016/j.jallcom.2020.157207>.
- [20] Selvaraj AR, Muthusamy A, In-ho-Cho, Kim HJ, Senthil K, Prabakar K. Ultrahigh surface area biomass derived 3D hierarchical porous carbon nanosheet electrodes for high energy density supercapacitors. *Carbon N Y* 2021;174:463–74. <https://doi.org/10.1016/j.carbon.2020.12.052>.
- [21] Zhang Y, Yu S, Lou G, Shen Y, Chen H, Shen Z, et al. Review of macroporous materials as electrochemical supercapacitor electrodes. *J Mater Sci* 2017;52:11201–28. <https://doi.org/10.1007/s10853-017-0955-3>.
- [22] Liu S, Li A, Han Q, Yang C, Li H, Xia H, et al. Oxygen-directed porous activation of carbon nanospheres for enhanced capacitive energy storage. *J Power Sources* 2021;483:229223. <https://doi.org/10.1016/j.jpowsour.2020.229223>.
- [23] Wang T, Xu Y, Shi B, Gao S, Meng G, Huang K. Novel activated N-doped hollow microporous carbon nanospheres from pyrrole-based hyper-crosslinking polystyrene for supercapacitors. *React Funct Polym* 2019;143:104326. <https://doi.org/10.1016/j.reactfunctpolym.2019.104326>.
- [24] Zheng L, Dai X, Ouyang Y, Chen Y, Wang X. nHighly N/O co-doped carbon nanospheres for symmetric supercapacitors application with high specific energy. *J Energy Storage* 2021;33:102152. <https://doi.org/10.1016/j.est.2020.102152>.
- [25] Zhou P, Wan J, Wang X, Xu K, Gong Y, Chen L. Nickel and cobalt metal-organic-frameworks-derived hollow microspheres porous carbon assembled from nanorods and nanospheres for outstanding supercapacitors. *J Colloid Interface Sci* 2020;575:96–107. <https://doi.org/10.1016/j.jcis.2020.04.083>.
- [26] He D, Gao Y, Wang Z, Yao Y, Wu L, Zhang J, et al. One-step green fabrication of hierarchically porous hollow carbon nanospheres (HCNSs) from raw biomass: formation mechanisms and supercapacitor applications. *J Colloid Interface Sci* 2021;581:238–50. <https://doi.org/10.1016/j.jcis.2020.07.118>.
- [27] Yaya A, Agyei-Tuffour B, Dodoo-Arhin D, Nyankson E, Annan E, Konadu DS, et al. Layered nanomaterials- A review. *Glob J Eng Des Technol* 2012;1:32–41.
- [28] Apriwandi A, Taer E, Farma R, Setiadi RN, Amiruddin E. A facile approach of micro-mesopores structure binder-free coin/monolith solid design activated carbon for electrode supercapacitor. *J Energy Storage* 2021;40:102823. <https://doi.org/10.1016/j.est.2021.102823>.
- [29] Liangshuo L, Lin Q, Xinyu L, Ming D, Xin F. Preparation of biomass-based porous carbon derived from waste ginger slices and its electrochemical performance. *Optoelectron Adv Mater Rapid Commun* 2020;14:548–55.
- [30] Gou H, He J, Zhao G, Zhang L, Yang C, Rao H. Porous nitrogen-doped carbon networks derived from orange peel for high-performance supercapacitors. *Ionics (Kiel)* 2019;25:4371–80. <https://doi.org/10.1007/s11581-019-02992-9>.
- [31] Brebu M, Vasile C. Thermal degradation of lignin – a review. *Cellul Chem Technol Cellul Chem Technol* 2009;44:353–63.
- [32] Zhang Q, Han K, Li S, Li M, Li J, Ren K. Synthesis of garlic skin-derived 3D hierarchical porous carbon for high-performance supercapacitors. *Nanoscale* 2018;10:2427–37. <https://doi.org/10.1039/c7nr07158b>.
- [33] Taer E, Handayani R, Apriwandi A, Taslim R, Awitdrus, Amri A, et al. The synthesis of bridging carbon particles with carbon nanotubes from areca catechu husk waste as supercapacitor electrodes. *Int J Electrochem Sci* 2019;14:9436–48. <https://doi.org/10.20964/2019.10.34>.
- [34] Erabee IK, Ahsan A, Zularisam AW, Idrus S, Daud NNN, Arunkumar T, et al. A new activated carbon prepared from sago palm bark through physiochemical activated process with zinc chloride. *Eng J* 2017;21:1–14. <https://doi.org/10.4186/ej.2017.21.5.1>.
- [35] Taslim R, Taer E, Siska M, Suedi, Suwandana, Agustino, et al. Synthesis of high porous activated carbon nanofibers using the single-step pyrolysis of reeds waste and its applications in supercapacitor electrodes. *Technol Reports Kansai Univ* 2020;62:5629–41.
- [36] Taer E, Apriwandi A, Taslim R, Malik U, Usman Z. Single step carbonization-activation of durian shells for producing activated carbon monolith electrodes. *Int J Electrochem Sci* 2019;14:1318–30. <https://doi.org/10.20964/2019.02.67>.
- [37] Girgis BS, Temerk YM, Gadelrab MM, Abdullah ID. X-ray diffraction patterns of activated carbons prepared under various conditions. *Carbon Sci* 2007;8:95–100. <https://doi.org/10.5714/cl.2007.8.2.095>.
- [38] Wang Y, Qiao M, Mamat X. Nitrogen-doped macro-meso-micro hierarchical ordered porous carbon derived from ZIF-8 for boosting supercapacitor performance. *Appl Surf Sci* 2021;540:148352. <https://doi.org/10.1016/j.apsusc.2020.148352>.
- [39] Taer E, Apriwandi, Dalimunthe BKL, Taslim R. A rod-like mesoporous carbon derived from agro-industrial cassava petiole waste for supercapacitor application. *J Chem Technol Biotechnol* 2021;96. <https://doi.org/10.1002/jctb.6579>.
- [40] Kumar K, Saxena RK, Kothari R, Suri DK, Kaushik NK, Bohra JN. Correlation between adsorption and x-ray diffraction studies on viscose rayon based activated carbon

- cloth. Carbon N Y 1997;35:1842–4. [https://doi.org/10.1016/S0008-6223\(97\)87258-2](https://doi.org/10.1016/S0008-6223(97)87258-2).
- [41] Deraman M, Daik R, Soltaninejad S, Nor NSM, Awitdrus A, Farma R, et al. A new empirical equation for estimating specific surface area of supercapacitor carbon electrode from X-ray diffraction. Adv Mater Res 2015;1108:1–7. <https://doi.org/10.4028/www.scientific.net/AMR.1108.1>.
- [42] Roy CK, Shah SS, Reaz AH, Sultana S, Chowdhury AN, Firoz SH, et al. Preparation of hierarchical porous activated carbon from banana leaves for high-performance supercapacitor: effect of type of electrolytes on performance. Chem Asian J 2021;16:296–308. <https://doi.org/10.1002/asia.202001342>.
- [43] Kuzmenko V, Naboka O, Haque M, Staaf H, Göransson G, Gatenholm P, et al. Sustainable carbon nanofibers/nanotubes composites from cellulose as electrodes for supercapacitors. Energy 2015;90:1490–6. <https://doi.org/10.1016/j.energy.2015.06.102>.
- [44] Hor AA, Hashmi SA. Optimization of hierarchical porous carbon derived from a biomass pollen-cone as high-performance electrodes for supercapacitors. Electrochim Acta 2020;356:136826. <https://doi.org/10.1016/j.electacta.2020.136826>.
- [45] Boyjoo Y, Cheng Y, Zhong H, Tian H, Pan J, Pareek VK, et al. From waste Coca Cola® to activated carbons with impressive capabilities for CO₂ adsorption and supercapacitors. Carbon N Y 2017;116:490–9. <https://doi.org/10.1016/j.carbon.2017.02.030>.
- [46] Azwar E, Wan Mahari WA, Chuah JH, Vo DVN, Ma NL, Lam WH, et al. Transformation of biomass into carbon nanofiber for supercapacitor application-A review. Int J Hydrogen Energy 2018;43:20811–21. <https://doi.org/10.1016/j.ijhydene.2018.09.111>.
- [47] Chinnadurai D, Kim HJ, Karupannan S, Prabakar K. Multiscale honeycomb-structured activated carbon obtained from nitrogen-containing Mandarin peel: high-performance supercapacitors with significant cycling stability. New J Chem 2019;43:3486–92. <https://doi.org/10.1039/C8NJ05895D>.
- [48] Duan B, Gao X, Yao X, Fang Y, Huang L, Zhou J, et al. Unique elastic N-doped carbon nanofibrous microspheres with hierarchical porosity derived from renewable chitin for high rate supercapacitors. Nanomater Energy 2016;27:482–91. <https://doi.org/10.1016/j.nanoen.2016.07.034>.
- [49] Taer E, Apriwandi A, Taslim R, Agutino A, Yusra DA. Conversion Syzygium oleana leaves biomass waste to porous activated carbon nanosheet for boosting supercapacitor performances. J Mater Res Technol 2020;9:13332–40. <https://doi.org/10.1016/j.jmrt.2020.09.049>.
- [50] Chen Y, Jiang Y, Liu Z, Yang L, Du Q, Zhuo K. Hierarchical porous N-doped graphene aerogel with good wettability for high-performance ionic liquid-based supercapacitors. Electrochim Acta 2021;366. <https://doi.org/10.1016/j.electacta.2020.137414>.
- [51] Contescu CI, Adhikari SP, Gallego NC, Evans ND. Activated carbons derived from high-temperature pyrolysis of lignocellulosic Biomass. J Carbon Res 2018;4:9–13. <https://doi.org/10.3390/c4030051>.
- [52] Yang V, Senthil RA, Pan J, Khan A, Osman S, Wang L, et al. Highly ordered hierarchical porous carbon derived from biomass waste mangosteen peel as superior cathode material for high performance supercapacitor. J Electroanal Chem 2019;113616. <https://doi.org/10.1016/j.jelechem.2019.113616>.
- [53] Ghosh S, Barg S, Jeong SM, Ostrikov K. Heteroatom-Doped and oxygen-functionalized nanocarbons for high-performance supercapacitors. Adv Energy Mater 2020;10:1–44. <https://doi.org/10.1002/aenm.202001239>.
- [54] Wang T, He X, Gong W, Sun K, Lu W, Yao Y, et al. Flexible carbon nano fibers for high-performance free-standing supercapacitor electrodes derived from Powder River Basin coal. Fuel 2020;278:117985. <https://doi.org/10.1016/j.fuel.2020.117985>.
- [55] Fu Y, Zhang N, Shen Y, Ge X, Chen M. Micro-mesoporous carbons from original and pelletized rice husk via one- step catalytic pyrolysis. Bioresour Technol 2018;269:67–73. <https://doi.org/10.1016/j.biortech.2018.08.083>.
- [56] Kumar TR, Senthil RA, Pan Z, Pan J, Sun Y. A tubular-like porous carbon derived from waste American poplar fruit as advanced electrode material for high-performance supercapacitor. J Energy Storage 2020;32:101903. <https://doi.org/10.1016/j.est.2020.101903>.

Solid coin-like design activated carbon nanospheres derived from shallot peel precursor for boosting supercapacitor performance

ORIGINALITY REPORT

15%

SIMILARITY INDEX

9%

INTERNET SOURCES

13%

PUBLICATIONS

%

STUDENT PAPERS

PRIMARY SOURCES

1

pure.unileoben.ac.at

Internet Source

1%

2

Erman Taer, Apriwandi, Agustino, Rika Taslim, Widya Sinta Mustika, Exa Fadli. "SURFACE MODIFICATION: UNIQUE ELLIPSOIDAL/STROBILI-FIBER STRUCTURE OF POROUS CARBON MONOLITH FOR ELECTRODE SUPERCAPACITOR", Nanoscience and Technology: An International Journal, 2021

Publication

1%

3

research.aalto.fi

Internet Source

1%

4

Chuanzheng Hu, Junhui Xu, Zhen Lu, Chunhua Cao, Yazhen Wang. "Core-shell structured ZIF-7@ZIF-67 with high electrochemical performance for all-solid-state asymmetric supercapacitor", International Journal of Hydrogen Energy, 2021

Publication

1%

5

Erman Taer, Aprilia Susanti, Rika Taslim, Apriwandi. "Renewable and environmentally friendly of "red shoots" leaves biomass-based carbon electrode materials for supercapacitor energy storage", Journal of Physics: Conference Series, 2021

Publication

1 %

6

curis.ku.dk

Internet Source

1 %

7

Li-Feng Chen, Xu-Dong Zhang, Hai-Wei Liang, Mingguang Kong, Qing-Fang Guan, Ping Chen, Zhen-Yu Wu, Shu-Hong Yu. "Synthesis of Nitrogen-Doped Porous Carbon Nanofibers as an Efficient Electrode Material for Supercapacitors", ACS Nano, 2012

Publication

1 %

8

pubs.rsc.org

Internet Source

<1 %

9

E. Taer, Apriwandi, R. Taslim, Agustino. "The effect of physical activation temperature on physical and electrochemical properties of carbon electrode made from jengkol shell (Pithecellobium jiringa) for supercapacitor application", Materials Today: Proceedings, 2021

Publication

<1 %

10

iopscience.iop.org

<1 %

11

Erman Taer, Nazilah Nikmatun, Apriwandi, Agustino, Rika Taslim, Ezri Hidayat. "The Self-Adhesive Carbon Powder Based on Coconut Coir Fiber as Supercapacitor Application", Journal of Metastable and Nanocrystalline Materials, 2021

Publication

<1 %

12

Abhishek Dhar, Nadavala Siva Kumar, Mehul Khimani, Ahmed S. Al - Fatesh et al. "Naturally occurring neem gum: An unprecedented green resource for bioelectrochemical flexible energy storage device", International Journal of Energy Research, 2019

Publication

<1 %

13

Maria Cecília Ramos de Araújo Veloso, Marina Rates Pires, Luciana Silva Villela, Mário Vanoli Scatolino et al. "Potential destination of Brazilian cocoa agro-industrial wastes for production of materials with high added value", Waste Management, 2020

Publication

<1 %

14

Zhigao Xue, Ling Lv, Ye Tian, Shiwen Tan, Qingxiang Ma, Kai Tao, Lei Han. " Co S Nanoplate Arrays Decorated with Oxygen-Deficient CeO Nanoparticles for

<1 %

Supercapacitor Applications ", ACS Applied Nano Materials, 2021

Publication

15

onlinelibrary.wiley.com

Internet Source

<1 %

16

Erman Taer, Friska Febriyanti, Apriwandi, Rika Taslim, Agustino, Widya Sinta Mustika. " Investigation of H SO and KOH aqueous electrolytes on the electrochemical performance of activated carbon derived from areca catechu husk ", Journal of Physics: Conference Series, 2021

Publication

<1 %

17

Antonio B. Fuertes, Marta Sevilla. "Hierarchical Microporous/Mesoporous Carbon Nanosheets for High-Performance Supercapacitors", ACS Applied Materials & Interfaces, 2015

Publication

<1 %

18

Li Zhao, Li-Zhen Fan, Meng-Qi Zhou, Hui Guan, Suyan Qiao, Markus Antonietti, Maria-Magdalena Titirici. "Nitrogen-Containing Hydrothermal Carbons with Superior Performance in Supercapacitors", Advanced Materials, 2010

Publication

<1 %

19

Min Luo, Ziqi Zhu, Kai Yang, Pei Yang, Yingchun Miao, Minzhi Chen, Weimin Chen,

<1 %

Xiaoyan Zhou. "Sustainable biomass-based hierarchical porous carbon for energy storage: A novel route to maintain electrochemically attractive natural structure of precursor", Science of The Total Environment, 2020

Publication

20

Ali Ehsani, Hamidreza Parsimehr. "Electrochemical energy storage electrodes from fruit biochar", Advances in Colloid and Interface Science, 2020

Publication

21

Erman Taer, Friska Febriyanti, Widya Sinta Mustika, Rika Taslim, Agustino Agustino, Apriwandi Apriwandi. "Enhancing the performance of supercapacitor electrode from chemical activation of carbon nanofibers derived Areca catechu husk via one-stage integrated pyrolysis", Carbon Letters, 2020

Publication

22

S. E. M. Pourhosseini, Omid Norouzi, Pejman Salimi, Hamid Reza Naderi. "Synthesis of a Novel Interconnected 3D Pore Network Algal Biochar Constituting Iron Nanoparticles Derived from a Harmful Marine Biomass as High-Performance Asymmetric Supercapacitor Electrodes", ACS Sustainable Chemistry & Engineering, 2018

Publication

<1 %

<1 %

<1 %

23

Sevilla, Marta, and Antonio B. Fuertes. "Direct Synthesis of Highly Porous Interconnected Carbon Nanosheets and Their Application as High-Performance Supercapacitors", ACS Nano

Publication

<1 %

24

Chunyan Li, Yaju Zhou, Pengwei Huo, Xinkun Wang. "Fabricated high performance ultrathin MoSe₂ nanosheets grow on MWCNT hybrid materials for asymmetric supercapacitors", Journal of Alloys and Compounds, 2020

Publication

<1 %

25

Erman Taer, Mega Ratna Dewi, Apriwandi, Rika Taslim, Agustino, Widya Sinta Mustika. "Study of the influence of different activator agents on the dimensions, mass, volume, and density of activated carbon monoliths for large-scale practical applications", Journal of Physics: Conference Series, 2021

Publication

<1 %

26

Luyi Chen, Bingna Zheng, Junlong Huang, Zhiwei Tang, Shaohong Liu, Ruliang Liu, Dingcai Wu, Ruowen Fu. "Fabrication of three-dimensionally nanostructured carbon materials with functional tube-in-tube network units for enhanced electrochemical performances", Carbon, 2019

Publication

<1 %

27	advances.sciencemag.org Internet Source	<1 %
28	mafiadoc.com Internet Source	<1 %
29	mdpi.com Internet Source	<1 %
30	www.science.gov Internet Source	<1 %
31	www.sciencegate.app Internet Source	<1 %
32	Keqi Qu, Yue You, Houjuan Qi, Cai Shi, Zhe Sun, Zhanhua Huang, Bingnan Yuan, Zhanhu Guo. "Fungus Bran-Derived Porous N-Doped Carbon–Zinc Manganese Oxide Nanocomposite Positive Electrodes toward High-Performance Asymmetric Supercapacitors", The Journal of Physical Chemistry C, 2020 Publication	<1 %
33	Liping Zheng, Xiaochao Dai, Yinhui Ouyang, Yulian Chen, Xianyou Wang. "nHighly N/O co-doped carbon nanospheres for symmetric supercapacitors application with high specific energy", Journal of Energy Storage, 2021 Publication	<1 %

34

Lu Luo, Yalan Zhou, Wen Yan, Lingcong Luo, Jianping Deng, Guanben Du, Mizi Fan, Weigang Zhao. "Design and construction of hierarchical sea urchin-like NiCo-LDH@ACF composites for high-performance supercapacitors", Industrial Crops and Products, 2021

Publication

<1 %

35

Raja Arumugam Senthil, Viengkham Yang, Junqing Pan, Yanzhi Sun. "A green and economical approach to derive biomass porous carbon from freely available feather finger grass flower for advanced symmetric supercapacitors", Journal of Energy Storage, 2021

Publication

<1 %

36

Xiaoyu Zheng, Wei Lv, Ying Tao, Jiaojing Shao, Chen Zhang, Donghai Liu, Jiayan Luo, Da-Wei Wang, Quan-Hong Yang. "Oriented and Interlinked Porous Carbon Nanosheets with an Extraordinary Capacitive Performance", Chemistry of Materials, 2014

Publication

<1 %

37

Yapeng He, Xue Wang, Panpan Zhang, Hui Huang, Xiaobo Li, Yuan Shui, Buming Chen, Zhongcheng Guo. "A versatile integrated rechargeable lead dioxide-polyaniline system

<1 %

with energy storage mechanism
transformation", Energy, 2019

Publication

38

agronomy.emu.ee

Internet Source

<1 %

39

dokumen.pub

Internet Source

<1 %

40

pt.scribd.com

Internet Source

<1 %

41

www.tandfonline.com

Internet Source

<1 %

42

Erman Taer, Apriwandi, Bima Kumala
Levanadea Dalimunthe, Rika Taslim. "A rod -
like mesoporous carbon derived from agro -
industrial cassava petiole waste for
supercapacitor application", Journal of
Chemical Technology & Biotechnology, 2020

Publication

<1 %

43

Leonardo M. Da Silva, Reinaldo Cesar, Cássio
M.R. Moreira, Jéferson H.M. Santos et al.
"Reviewing the fundamentals of
supercapacitors and the difficulties involving
the analysis of the electrochemical findings
obtained for porous electrode materials",
Energy Storage Materials, 2020

Publication

<1 %

44

Zhibin Yang, Jing Ren, Zhitao Zhang, Xuli Chen, Guozhen Guan, Longbin Qiu, Ye Zhang, Huisheng Peng. "Recent Advancement of Nanostructured Carbon for Energy Applications", Chemical Reviews, 2015

Publication

<1 %

45

Dian Andriani, Arina Yuthi Apriyana, Myrtha Karina. "The optimization of bacterial cellulose production and its applications: a review", Cellulose, 2020

Publication

<1 %

46

Erman Taer, Apriwandi Apriwandi, Bima Kumala Levanadea Dalimunthe, Rika Taslim. "A rod - like mesoporous carbon derived from agro - industrial cassava petiole waste for supercapacitor application", Journal of Chemical Technology & Biotechnology, 2020

Publication

<1 %

47

Jianxiong Xu, Guo Du, Lei Xie, Kai Yuan, Yirong Zhu, Lijian Xu, Na Li, Xianyou Wang. "Three-Dimensional Walnut-Like, Hierarchically Nanoporous Carbon Microspheres: One-Pot Synthesis, Activation, and Supercapacitive Performance", ACS Sustainable Chemistry & Engineering, 2020

Publication

<1 %

48

Juan Du, Lei Liu, Zepeng Hu, Yifeng Yu, Yue Zhang, Senlin Hou, Aibing Chen. "Raw-Cotton-

<1 %

Derived N-Doped Carbon Fiber Aerogel as an Efficient Electrode for Electrochemical Capacitors", ACS Sustainable Chemistry & Engineering, 2018

Publication

49

Kateryna Bazaka, Mohan V. Jacob, Kostya (Ken) Ostrikov. "Sustainable Life Cycles of Natural-Precursor-Derived Nanocarbons", Chemical Reviews, 2015

Publication

<1 %

50

Yujuan Cao, Wu Yang, Mingyue Wang, Ning Wu, Longwen Zhang, Qixia Guan, Hao Guo. "Metal-organic frameworks as highly efficient electrodes for long cycling stability supercapacitors", International Journal of Hydrogen Energy, 2021

Publication

<1 %

51

Zhong, Cheng, Yida Deng, Wenbin Hu, Daoming Sun, Xiaopeng Han, Jinli Qiao, and Jiujun Zhang. "Electrolytes for Electrochemical Supercapacitors", Electrochemical Energy Storage and Conversion, 2016.

Publication

<1 %

Exclude quotes On

Exclude matches Off

Exclude bibliography On